20-Gbit/s direct modulation of GaInAsP/InP membrane distributed-reflector laser with energy cost of less than 100 fJ/bit

OPEN ACCESS
Applied Physics Express **11**, 012704 (2018)
https://doi.org/10.7567/APEX.11.012704

20-Gbit/s direct modulation of GaInAsP/InP membrane distributed-reflector laser with energy cost of less than 100 fJ/bit

Takahiro Tomiyasu[1], Daisuke Inoue[1], Takuo Hiratani[1], Kai Fukuda[1], Nagisa Nakamura[1], Tatsuya Uryu[1], Tomohiro Amemiya[1,2], Nobuhiko Nishiyama[1,2], and Shigehisa Arai[1,2*]

[1]*Department of Electrical and Electronic Engineering, Tokyo Institute of Technology, Meguro, Tokyo 152-8552, Japan*
[2]*Institute of Innovative Research, Tokyo Institute of Technology, Meguro, Tokyo 152-8552, Japan*

*E-mail: arai@pe.titech.ac.jp

Received November 15, 2017; accepted December 4, 2017; published online December 19, 2017

We demonstrated 20-Gbit/s direct modulation with a low energy cost of the membrane distributed-reflector (DR) laser whose static lasing characteristics were previously reported by Tomiyasu et al. in Appl. Phy. Express **10**, 062702 (2017). As a small-signal modulation characteristic, a modulation current efficiency of 12 GHz/mA$^{1/2}$ was obtained. In 20-Gbit/s direct modulation using a non-return-to-zero $2^{11} - 1$ word-length pseudorandom bit sequence signal, a clear eye opening with a bit-error rate of 6.4×10^{-10} was obtained with a bias current of 1.06 mA and a bias voltage of 1.76 V, which resulted in a record low energy cost of 93 fJ/bit among membrane distributed-feedback (DFB) and DR lasers ever reported. © 2018 The Japan Society of Applied Physics

For decades, the performance of Si large-scale integrated circuits (LSIs) has been progressively improved with downscaling.[1)] However, the increase in the speed of data transmission and global wire layers has reached the performance limitations of LSIs owing to RC delays and large power dissipation in global wire layers.[2,3)] The introduction of high-speed optical data transmission with ultralow power consumption for on-chip interconnections can be an attractive solution to overcoming these problems. Many optical devices with Si photonics technology have been demonstrated because of their small footprints and low fabrication costs resulting from their high index contrast and compatibility with the complementary metal–oxide–semiconductor (CMOS) fabrication process.[4,5)] Several approaches have been developed for integrating III–V devices on Si substrates with highly crystalline III–V semiconductor layers such as direct wafer bonding, heteroepitaxial growth, and benzocyclobutene (BCB) bonding.[6–8)]

In addition, a semiconductor laser with ultralow power consumption is needed for the extensive replacement of electrical interconnections with optical interconnections. The available energy consumption for on-chip optical interconnections should be approximately 100 fJ/bit or less;[9)] that is, a power consumption less than 1 mW is required at a data rate of 10 Gbit/s. Several research groups have investigated the low-power-dissipation operations of vertical-cavity surface-emitting lasers (VCSELs),[10–12)] microdisk lasers,[13,14)] and photonic crystal lasers (PC-LDs).[15–17)] Although VCSELs have been introduced into short-reach board-to-board optical communication at datacenters and supercomputers owing to their potential for high-speed direct modulation with low energy consumption,[18)] 45° total-reflection mirrors are required to establish in-plane integrated circuits with VCSELs.[19)] Microdisk lasers and PC-LDs have demonstrated low-energy-cost data transmission in in-plane optical links.

We have proposed membrane distributed-feedback (DFB) and distributed-reflector (DR) lasers as high-efficiency light sources with ultralow power consumption for on-chip optical interconnections and membrane photonic integrated circuits (MPICs).[20–22)] The semiconductor membrane structure, consisting of a thin (250–400 nm) semiconductor layer sandwiched by low-refractive-index dielectric cladding layers or air, can enhance the optical confinement into the active layer. Consequently, low-threshold-current operation and small-footprint devices can be realized owing to the high optical modal gain and high index-coupling coefficient of the grating in the DFB and distributed-Bragg-reflector (DBR) structures. The DR structure enables the increase in light output at one side owing to the high reflectivity of the DBR structure at the opposite side. Therefore, membrane lasers, especially membrane DR lasers, are expected to be one of the promising light sources for on-chip optical interconnections.

Recently, we have demonstrated a low threshold current and high-efficiency operation with membrane DR lasers bonded on a Si substrate by using benzocyclobutene (BCB) polymer.[23)] Moreover, continuous-wave (CW) operation up to 90 °C[24)] and 10-Gbits/s direct modulation with a modulation current efficiency factor (MCEF) of 7.9 GHz/mA$^{1/2}$ were demonstrated.[25)] After the investigation of drastic waveguide loss reduction,[26)] we obtained a membrane DR laser with high external differential quantum efficiency as well as high power-conversion efficiency.[27,28)]

In this paper, we report high-speed direct modulation of the membrane DR laser whose structure, fabrication process, and static lasing characteristics were reported in a previous paper.[27)] The fabricated device has 32-µm-long DFB and 50-µm-long DBR sections, and a 0.8 µm stripe width, as shown in Fig. 1(a), and an active region consisting of five GaInAsP strained quantum wells sandwiched by InP layers with a total thickness of 270 nm. These InP layers prevent nonradiative recombination on surface GaInAsP layers. In order to achieve high-efficiency operation, we reduced the doping concentration of the p-InP side cladding layer and shortened the distance between the edges of the p-side electrode and the active section. Since a high doping concentration of 2×10^{18} cm^{-3} of the p-InP side cladding layer resulted in a high waveguide loss of 42 cm^{-1} in our previous works,[29)] we reduced the doping concentration of the p-side cladding layer to 5×10^{17} cm^{-3} and obtained a waveguide loss of 22 cm^{-1}.[26)] However, this reduction in the doping concentration causes an increase in the series resistance between the p-side electrode and the active section. Therefore, the distance between the edge of the p-side electrode and the active section was reduced from 3 to 1.6 µm.[27)] Moreover, the BCB thickness was reduced from 2 µm to approximately 500 nm to lower the thermal resistance. From a simulation of the thermal

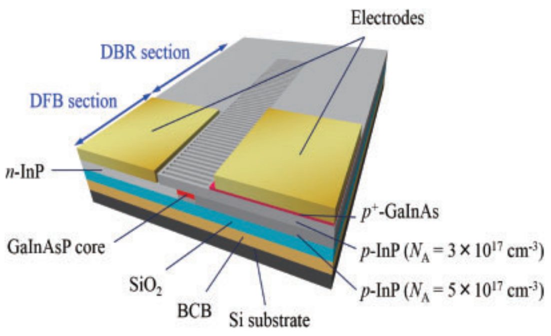

(a)

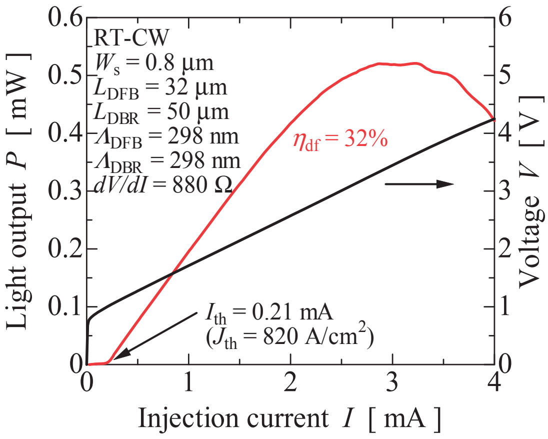

(b)

Fig. 1. (a) Schematic of the membrane DR laser. (b) Current–light and current–voltage characteristics.

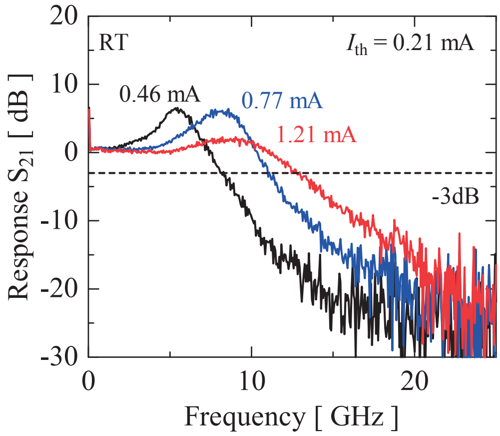

(a)

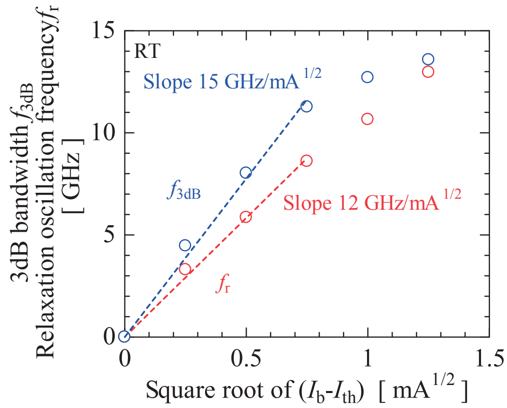

(b)

Fig. 2. Results of small-signal modulation measurement: (a) responses of S_{21} measured under various bias current conditions and (b) plots of relaxation oscillation frequency and 3-dB bandwidth versus square root of bias current above threshold.

resistance of the device structure, these changes will reduce the thermal resistance from 3400 to 2000 K/W.

Figure 1(b) shows the light–current (L–I) and current–voltage (I–V) characteristics of the device under RT–CW conditions. The power was measured with a 10-mm-diameter GaInAs photodiode with National Institute of Standards and Technology (NIST) traceable calibration. The threshold current was as low as $I_{th} = 0.21$ mA, corresponding to a threshold current density J_{th} of 820 A/cm^2. The light output increased linearly with the injection current, showing an external differential quantum efficiency for front-side output, η_{df}, of 32%, up to an injection current of approximately 1.5 mA. The maximum output power was 0.52 mW when the injection current was increased to 3.2 mA. Compared with our previously reported membrane DR lasers that operated up to 90 °C under a CW condition and for which thermal roll-off was observed at around 2.2 mA,[24] a higher CW operation temperature can be expected. Actually, high-temperature CW operation (100 °C) and high-speed modulation (25.8 Gbit/s) of membrane DFB lasers directly bonded on SiO_2/Si substrates have been reported,[30] where the thermal resistance was estimated to be around 700 K/W for the active region length of 73 μm. A low threshold current and high-differential-quantum-efficiency operation were achieved owing to the reduction in waveguide loss. The differential series resistance dV/dI and the voltage at the threshold current, V_{th}, were 880 Ω and 1.0 V, respectively. The differential series resistance of 880 Ω is close to the value of 740 Ω achieved with almost the same cavity length in a previous work,[25] because the resistance increase due to the effect of the low-doped p-InP side cladding layer was compensated by shortening the distance between the p-side electrode and the active section.

The direct modulation characteristics of the device were determined from the small-signal modulation response and 20-Gbit/s large-signal modulation. First, the small-signal response was measured using a vector network analyzer (VNA). An electrical modulation signal was applied to the device via a 40 GHz high-speed ground-signal (GS) RF probe with a 100 μm pitch. The optical output signal was coupled to a spherical-lens single-mode fiber. Finally, the collected optical signal was detected with a 20-GHz PIN-trans-impedance amplifier (TIA) photoreceiver. From the measurement of the electrical transmission characteristics of S_{21} and S_{11} using a DFB laser with the same structure, the bandwidth limited by the RC constant f_{RC} of the device was found to be about 13.7 GHz. Since the relaxation oscillation frequency f_r measured from the relative intensity noise (RIN) coincided with that determined by small-signal response measurement,[31] S_{21} for bias currents ranging from 0.46 to 1.21 mA was found to be as shown in Fig. 2(a). As the bias current was increased to 1.21 mA, both f_r and the 3-dB bandwidth f_{3dB} increased. At a bias current of 0.77 mA, f_{3dB} reached 11.2 GHz, which implies that not only 10-Gbit/s operation but also 15-Gbit/s operation can be expected with a bias

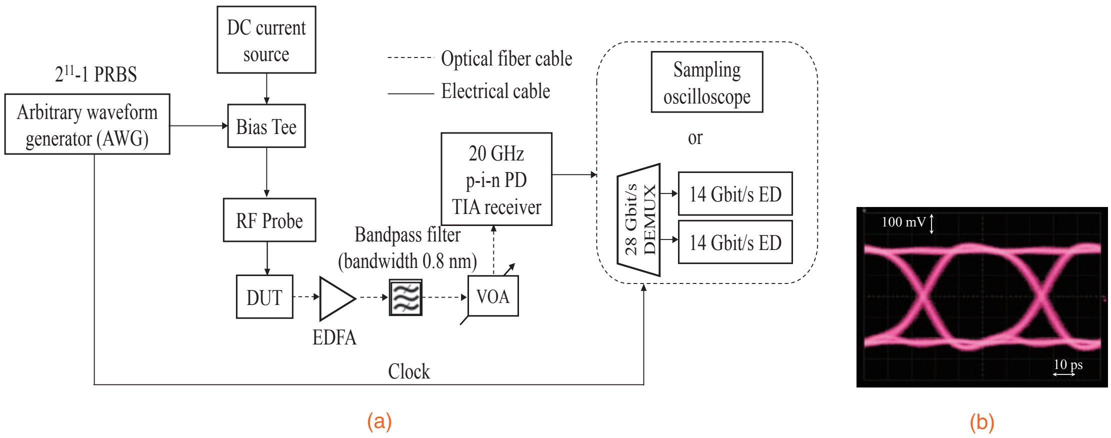

Fig. 3. Large-signal modulation of membrane DR laser: (a) measurement setup and (b) 20-Gbit/s electrical input signal to the device.

current of approximately 1.0 mA. The maximum f_{3dB} of 13.6 GHz was obtained at a bias current of 1.77 mA. From the small-signal modulation response, f_r and f_{3dB} were obtained as functions of the square root of bias current above the threshold current, as shown in Fig. 2(b). The slopes of f_r (MCEF) and f_{3dB} were 12 and 15 GHz/mA$^{1/2}$, respectively. The MCEF of 12 GHz/mA$^{1/2}$ is slightly higher than the value of 11 GHz/mA$^{1/2}$ previously reported for a membrane DFB laser with the DFB section length of 50 μm.[32)]

Finally, 20-Gbit/s large-signal direct modulation and bit-error-rate (BER) measurements were performed. Figure 3(a) shows the measurement setup. An electrical data signal of the non-return-to-zero (NRZ) modulation scheme with a $2^{11} - 1$ word-length pseudorandom bit sequence (PBRS) was generated by an arbitrary waveform generator. Figure 3(b) shows the 20-Gbit/s electrical input signal to the device. The optical output was amplified by an Er-doped fiber amplifier (EDFA), and the amplified spontaneous emission (ASE) was filtered by a tunable bandpass filter. The amplified optical power was monitored and attenuated using a variable optical attenuator before the 20-GHz PIN-TIA photoreceiver.

Figure 4(a) shows the BER characteristics of the membrane DR laser at a data rate of 20 Gbit/s as a function of average received power. The bias current for the device and modulation voltage swing were set to 1.06 mA and 0.45 V_{pp}, respectively. The minimum BER of 6.4×10^{-10} was obtained at an average received power of −4.8 dBm, which was slightly higher than that in our previous work on the membrane DFB laser (−6 dBm for a BER of 10^{-9} at 10 Gbit/s).[32)] This result demonstrates the feasibility of using the membrane DR laser as a light source with ultralow power consumption for on-chip optical interconnections. Figure 4(b) shows the 20-Gbit/s eye diagram measured at an average received power of −4.8 dBm. As can be seen, the eye opening was confirmed. Noise was moderately suppressed because the absorption section at the rear of the device prevented signal reflection back to the cavity. From a bias voltage of 1.76 V at an injection current of 1.06 mA, the energy cost for this modulation was obtained as 93 fJ/bit. To the best of our knowledge, this is the lowest value reported for membrane DFB and DR lasers. A low energy cost of 97 fJ/bit under 25.8 Gbit/s modulation was demonstrated for a similar DR laser bonded on a SiO_2/Si substrate, which had a differential resistance of less than 80 Ω and was biased at only 1.04 V.[33,34)] If we can reduce the differential resistance and the bias voltage similarly, the energy cost can be reduced to around 55 fJ/bit (at 20 Gbit/s).

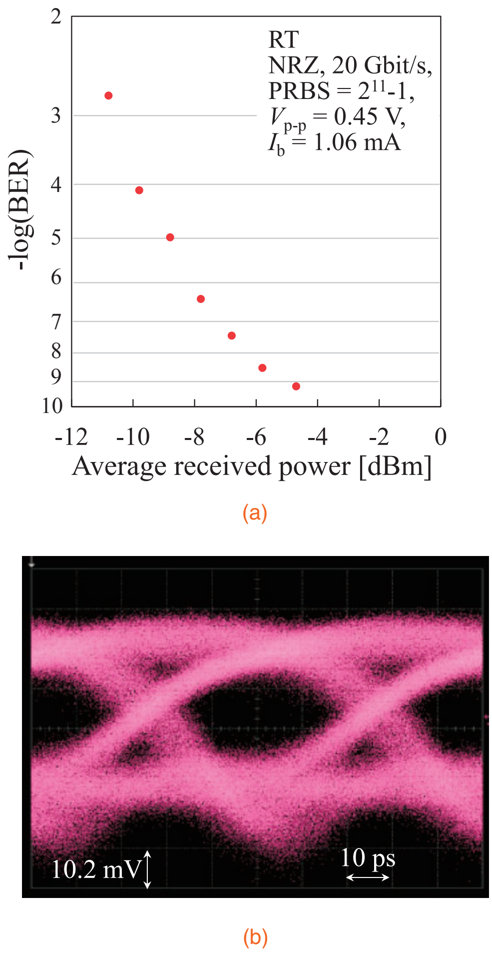

Fig. 4. Results of large-signal modulation measurement: (a) 20-Gbit/s BER characteristics and (b) eye diagram at a BER of 6.4×10^{-10}.

In conclusion, we have demonstrated the high-speed direct modulation of a membrane DR laser with a threshold current of 0.21 mA, an external differential quantum efficiency of 32%, and a maximum power conversion efficiency of 12.5%. A high modulation current efficiency of 12 GHz/mA$^{1/2}$, a minimum BER of 6.4×10^{-10}, and an energy cost of 93 fJ/bit were obtained for a data rate of 20 Gbit/s with a bias current as low as 1.06 mA and a modulation voltage of 0.45 V_{pp}. These results show that the membrane DR laser is a feasible light source for on-chip optical interconnections.

Acknowledgments The authors would like to thank Professors S. Akiba, T. Mizumoto, M. Asada, Y. Miyamoto, M. Watanabe, and Y. Shoji of the Tokyo Institute of Technology for fruitful discussions and comments. This work was supported by JSPS KAKENHI Grant Numbers 15H05763, 16H06082, 17H03247, and by JST-CREST Grant Number JPMJCR15N6.

1) R. H. Dennard, F. H. Gaensslen, V. L. Rideout, E. Bassous, and A. R. LeBlanc, IEEE J. Solid-State Circuits **9**, 256 (1974).
2) P. Kapur, J. P. McVittie, and K. C. Saraswat, IEEE Trans. Electron Devices **49**, 590 (2002).
3) P. Kapur, G. Chandra, J. P. McVittie, and K. C. Saraswat, IEEE Trans. Electron Devices **49**, 598 (2002).
4) N. Ophir, K. Padmaraju, A. Biberman, L. Chen, K. Preston, M. Lipson, and K. Bergman, Optical Fiber Communication Conf., 2011, OWZ3.
5) L. C. Kimerling, D. L. Kwong, and K. Wada, MRS Bull. **39**, 687 (2014).
6) D. Liang, M. Fiorentino, T. Okumura, H. H. Chang, D. T. Spencer, Y. Ha. Kuo, A. W. Fang, D. Dai, R. G. Beausoleil, and J. E. Bowers, Opt. Express **17**, 20355 (2009).
7) A. Y. Liu, C. Zhang, J. Norman, A. Snyder, D. Lubyshev, J. M. Fastenau, A. W. K. Liu, A. C. Gossard, and J. E. Bowers, Appl. Phys. Lett. **104**, 041104 (2014).
8) G. Roelkens, J. Brouckaert, D. V. Thourhout, R. Baets, R. Nötzel, and M. Smit, J. Electrochem. Soc. **153**, G1015 (2006).
9) D. A. B. Miller, Proc. IEEE **97**, 1166 (2009).
10) S. Imai, K. Takaki, S. Kamiya, H. Shimizu, J. Yoshida, Y. Kawakita, T. Takagi, K. Hiraiwa, H. Shimizu, T. Suzuki, N. Iwai, T. Ishikawa, N. Tsukiji, and A. Kasukawa, IEEE J. Sel. Top. Quantum Electron. **17**, 1614 (2011).
11) A. Kasukawa, IEEE Photonics J. **4**, 642 (2012).
12) P. Moser, J. A. Lott, P. Wolf, G. Larisch, H. Li, N. N. Ledentsov, and D. Bimberg, Electron. Lett. **48**, 1292 (2012).
13) M. Fujita, R. Ushigome, and T. Baba, Electron. Lett. **36**, 790 (2000).
14) J. Van Campenhout, P. Rojo-Romeo, P. Regreny, C. Seassal, D. Van Thourhout, S. Verstuyft, L. D. Cioccio, J.-M. Fedeli, C. Lagahe, and R. Beaets, Opt. Express **15**, 6744 (2007).
15) S. Matsuo, A. Shinya, T. Kakitsuka, K. Nozaki, T. Segawa, T. Sato, Y. Kawaguchi, and M. Notomi, Nat. Photonics **4**, 648 (2010).
16) B. Ellis, M. A. Mayer, G. Shambat, T. Sarmiento, J. Harris, E. E. Haller, and J. Vučković, Nat. Photonics **5**, 297 (2011).
17) S. Matsuo, K. Takeda, T. Sato, M. Notomi, A. Shinya, K. Nozaki, H. Taniyama, K. Hasebe, and T. Kakitsuka, Opt. Express **20**, 3773 (2012).
18) P. K. Shen, C. T. Chen, R. H. Chen, S. S. Lin, C. C. Chang, H. L. Hsiao, H. C. Lan, Y. C. Lee, Y. S. Lin, and M. L. Wu, IEEE Photonics Technol. Lett. **27**, 1359 (2015).
19) H. Liu, C. F. Lam, and C. Johnson, Proc. 2010 18th IEEE Annu. Symp. High Performance Interconnects, 2010, p. 113.
20) T. Okamoto, N. Nunoya, Y. Onodera, S. Tamura, and S. Arai, Electron. Lett. **37**, 1455 (2001).
21) S. Arai, N. Nishiyama, T. Maruyama, and T. Okumura, IEEE J. Sel. Top. Quantum Electron. **17**, 1381 (2011).
22) T. Hiratani, T. Shindo, K. Doi, Y. Atsuji, D. Inoue, T. Amemiya, N. Nishiyama, and S. Arai, IEEE J. Sel. Top. Quantum Electron. **21**, 299 (2015).
23) T. Hiratani, D. Inoue, T. Tomiyasu, Y. Atsuji, K. Fukuda, T. Amemiya, N. Nishiyama, and S. Arai, Appl. Phys. Express **8**, 112701 (2015).
24) T. Hiratani, D. Inoue, T. Tomiyasu, K. Fukuda, T. Amemiya, N. Nishiyama, and S. Arai, Appl. Phys. Express **10**, 032702 (2017).
25) T. Hiratani, D. Inoue, T. Tomiyasu, K. Fukuda, T. Amemiya, N. Nishiyama, and S. Arai, IEEE J. Sel. Top. Quantum Electron. **23**, 3700108 (2017).
26) T. Tomiyasu, T. Hiratani, D. Inoue, N. Nakamura, T. Amemiya, N. Nishiyama, and S. Arai, Jpn. J. Appl. Phys. **56**, 050311 (2017).
27) T. Tomiyasu, T. Hiratani, D. Inoue, N. Nakamura, K. Fukuda, T. Uryu, T. Amemiya, N. Nishiyama, and S. Arai, Appl. Phys. Express **10**, 062702 (2017).
28) T. Hiratani, D. Inoue, T. Tomiyasu, K. Fukuda, N. Nakamura, T. Amemiya, N. Nishiyama, and S. Arai, IEEE Photonics Technol. Lett. **29**, 1832 (2017).
29) D. Inoue, J. Lee, K. Doi, T. Hiratani, Y. Atsuji, T. Amemiya, N. Nishiyama, and S. Arai, Appl. Phys. Express **7**, 072701 (2014).
30) S. Matsuo, T. Fujii, K. Hasebe, K. Takeda, T. Sato, and T. Kakitsuka, J. Lightwave Technol. **33**, 1217 (2015).
31) D. Inoue, T. Hiratani, K. Fukuda, T. Tomiyasu, T. Amemiya, N. Nishiyama, and S. Arai, Opt. Express **23**, 29024 (2015).
32) D. Inoue, T. Hiratani, K. Fukuda, T. Tomiyasu, T. Amemiya, N. Nishiyama, and S. Arai, Opt. Express **24**, 18571 (2016).
33) H. Nishi, T. Fujii, K. Takeda, K. Hasebe, T. Kakitsuka, T. Tsuchizawa, T. Yamamoto, K. Yamada, and S. Matsuo, Opt. Express **24**, 18346 (2016).
34) T. Fujii, K. Takeda, E. Kanno, K. Hasebe, H. Nishi, R. Nakao, T. Yamamoto, T. Kakitsuka, and S. Matsuo, 42nd European Conf. Exhib. Optical Communications, 2016, p. 734.